

OBSERVATION OF HUNGA TONGA VOLCANIC ERUPTION USING HYPERSPECTRAL INFRARED SATELLITE SENSORS

Xiaozhen Xiong¹, Xu Liu¹, Wan Wu^{1,2},
Qiguang Yang^{1,2}, Liqiao Lei^{1,2}, Daniel K. Zhou¹, Allen M. Larar¹

¹NASA Langley Research Center, Hampton, Virginia, 23681, USA
²Adnet Systems Inc., Bethesda, MD 20817, USA

ABSTRACT

The Hunga Tonga-Hunga Ha'apai volcanic eruption, with the largest eruption occurred on 15 January 2022, injected unprecedented amounts of water vapor (H_2O) and SO_2 to the stratosphere. Using the hyperspectral infrared sounder CrIS we present some unique features of the spectral near $9.6\ \mu\text{m}$ and its great potential value for detecting plume or clouds with the tops above tropopause. It is found the existence of two umbrella clouds and the propagation of the upper plume even in 8-9 hour after the eruption. Using a new Single Field-of-view Sounder Atmospheric Products (SiFSAP) from CrIS and ATMS on JPSS-1 that has a high spatial resolution of about 14 km, this study analyzes the impact of Hunga Tonga eruption on the distribution of H_2O and ozone, particularly the unprecedented ejection of water vapor in the stratosphere. These results demonstrate the value of hyperspectral infrared sounder and single-field-view products for monitoring the volcanic eruption and studying its impact to climate.

Index Terms— Water Vapor, Ozone, Plume, umbrella clouds, CrIS

1. INTRODUCTION

After experiencing two major eruptions of Hunga Tonga-Hunga Ha'apai (HTHH) volcano (175.38°W , 20.57°S) on 19 December 2021 (20:35 UTC) and 13 January 2022 (15:20 UTC), the most highly explosive eruption of HTHH occurred on 15 January 2022 (between 04:00-04:10 UTC), which overshoots the tops of plume to the lower mesosphere of ~ 55 km [1]. In addition to a large amount ejection of SO_2 , an exceptional feature from this submarine volcano is the unprecedented ejection of water vapor (in both magnitude and altitudes), which may need to take several years for the H_2O plume to dissipate [2]. With a pronounced and persistent sulfate aerosol layer formed near the mid-stratosphere formed and the excess water plume, this eruption has a large impact on stratospheric temperature, O_3 and climate [3][4].

Space-born thermal infrared sounders, like Atmospheric Infrared Sounder (AIRS), Infrared Atmospheric

Infrared Sounder Interferometer (IASI) and Cross-track Infrared Sounder (CrIS) have been used to retrieve atmospheric temperature, water vapor, O_3 and other trace gases. However, the current operational Level 2 algorithms for AIRS and CrIS, including the NOAA Unique Combined Atmospheric Processing System (NUCAPS) [6], and the Community Long-term Infrared Microwave Coupled Product System (CLIMCAPS) [7], one operational sounder product at NASA, all use 3×3 Field-of-View (FOVs) (along track \times across track) of hyperspectral measurements to derive a single 'cloud-cleared' spectrum, thereby resulting in products with a coarser resolution of about 45 km. On the contrary, the SFOV retrieval algorithm developed at NASA Langley research center uses the originally measured radiance in each FOV, and through an optimal estimation method to retrieve cloud parameters (cloud height, optical depth and effective radius) simultaneously with the atmospheric parameters, providing observation of temperature, water vapor, O_3 and cloud properties with a spatial resolution of 14 km at nadir. These SFOV products will be used for analysis in this study.

Two layers of umbrella clouds following the eruption on 15 January were identified using Himawari-8 geostationary satellite data, with the upper one at ~ 31 km and the lower one 17 km [8]. The overpasses of JPSS-1 (or NOAA-20) at 12:30 UTC and the overpass S-NPP at $\sim 13:20$ UTC just have a good snapshot to capture the volcano plume and umbrella clouds. This study will first analyze the special feature of the CrIS spectra of these cloud and its use for quantifying the cloud top heights, followed by using the CrIS SFOV retrieved products, i.e. the Single Field-of-view Sounder Atmospheric Products (SiFSAP), to analyze the impact of volcano eruption on the temperature, water vapor, clouds and O_3 .

2. DATA AND METHOD

CrIS is a Fourier transform spectrometer covering the long-wave ($655\text{--}1095\ \text{cm}^{-1}$), mid-wave ($1210\text{--}1750\ \text{cm}^{-1}$), and

short-wave ($2155\text{--}2550\text{ cm}^{-1}$) infrared spectral regions, with a spectral resolution of 0.625 cm^{-1} and 2211 channels in total in its full spectral resolution mode. It is an across-track scanning instrument with a 2200 km swath width, with the total angular field of view consisting of a 3×3 array of circular pixels of 14 km diameter each (nadir spatial resolution), providing twice daily global measurement with the mean local daytime overpass time in 13:30 in the ascending node, and a mean local nighttime overpass time in 01:30 in the descending node [9]. Both the L1B data from CrIS on Suomi National Polar-orbiting Partnership Project (SNPP) and JPSS-1 will be used to show the spectral feature of umbrella clouds, but the SiFSAP used in this study is only produced using CrIS and ATMS onboard on JPSS-1. The SiFSAP retrieval algorithm is based on the Principal Component-based Radiative Transfer Model (PCRTM) and an optimal estimation retrieval method (PCRTM-RA) [10]. Use of the PCRTM allows for fast and accurate calculations for thousands of spectral channels under all-sky conditions. The use of principal component (PC) to compress information from all spectral channels into the PC domain further enables to reduce the observational noise and use the information from all spectral channels in CrIS measurements. An optimal estimation method is applied to do the retrieval on PC-domain to derive temperature, water vapor, trace gases, cloud and surface parameters simultaneously. This algorithm has been successfully applied to AIRS and IASI data [7], and was recently applied to CrIS data [11].

Two reanalysis products are also used for analysis. One is the NASA Modern-Era Retrospective Analysis for Research and Applications, Version 2 (MERRA-2), which has a spatial resolution of $0.5^\circ \times 0.625^\circ$ latitude-by-longitude grid with a 3-h interval and 72 model layers up to 0.01 hPa. Another is ERA-5, which has a resolution of $0.25^\circ \times 0.25^\circ$ latitude-by-longitude grid with a 1-h interval. To match up two reanalysis data with CrIS measurements, the differences between the models and CrIS in both temporal and spatial domains have been taken into account. To account for temporal difference, a linear interpolation was first made between the 3-h interval of the MERRA-2 reanalysis data and the 1-h interval between the ERA-5 reanalysis data bounding the CrIS observation, then it was interpolated to the center of each FOV of CrIS to match up the model data with CrIS observation.

3. RESULTS

3.1. Spectral of volcano umbrella cloud and its use for cloud height detection

Using Himawari-8 data Gupta et al. (2023) identified two umbrella clouds at distinct elevations on 15 January, i.e. after 05:30 UTC, the strong westward propagation of an

upper umbrella (UB) cloud at $31\text{ km} \pm 1\text{--}3\text{ km}$ enabled the visibility of the lower umbrella (UA) cloud at $17\text{ km} \pm 1\text{--}2\text{ km}$. As shown from the brightness temperature (BT) at $11.1\text{ }\mu\text{m}$ in Figure 1, S-NPP at 13:20 UTC and JPSS-1 at 12:30 UTC captured the area with volcano umbrella clouds very well. Even the observation from CrIS on S-NPP and J-1 is about 4-5 hours behind the observation shown by Gupta et al.(2023) (see their Figure 1), two layers of umbrella clouds are still visible, and the area of lower umbrella clouds is nearly half of total area of clouds, which is larger than what is shown by Gupta et al.(2023) and is as expected due to the westward propagation.

Right panel shows some examples of spectra, with one for the upper umbrella (UA) cloud, lower umbrella (UB) cloud and clear sky (C), respectively. The spectra of upper and lower umbrella clouds (in both J-1 and S-NPP) have a few common features: (1) the difference of BT among 11, 12 and $13\text{ }\mu\text{m}$ is very small, confirming that they are very thick clouds; (2) they are very smooth from 750 to 990 cm^{-1} and the weak water absorption lines within this spectral range are almost invisible, which is contrary to the spectral of clear sky (C) that shows water absorption lines; (3) the upside down “U” shape near O_3 absorption band at $9.6\text{ }\mu\text{m}$. The characteristics of (2) and (3) indicate the cloud top is near or above tropopause where the water vapor is very low. As the temperature increases with altitude in the stratosphere, the BTs for those channels near the O_3 absorption peak tend to be higher, forming the upside down “U” shape, which is opposite to the “U” shape near $9.6\text{ }\mu\text{m}$ for clear sky (C) or over low clouds. This unique spectral near $9.6\text{ }\mu\text{m}$ can be used to detect the clouds at higher altitude layer above tropopause. More investigation based on radiative transfer simulation and validation of this method for other cases is on-going.

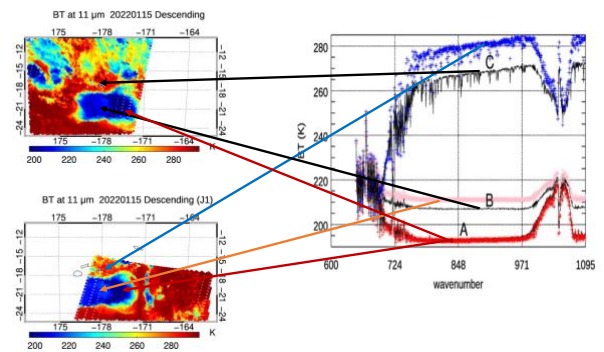


Figure 1 Map of BT at $11.1\text{ }\mu\text{m}$ from CrIS on S-NPP (13:20 UTC, upper left) and JPSS-1 (12:30 UTC, lower left), and examples of spectra corresponding to the upper umbrella (UA) cloud, lower umbrella (UB) cloud and clear sky (C) (right panel).

Using the Satellite Infrared Spectrometer (SIRS) flown on Nimbus 4, Ghazi [12] [13] first found that the SIRS radiance center at 678 cm^{-1} is highly correlated with the mean temperature of stratospheric layer at 100-5 mb (approximately 16-36 km). Figure 2 plots the brightness temperature (BT) measured by a CrIS stratospheric sounding channel at 678.25 cm^{-1} , and obviously the location of the warm air over the upper umbrella clouds center is evident. Using another stratospheric sounding channel at 691 cm^{-1} , which measures thermal radiance from a lower layer than 678.25 cm^{-1} , the warming center is still evident, confirming the westward and upward propagation of volcanic plume and the thick and highest plume is located near the northwest of the volcano. However, if using the BT at channel 668.125 cm^{-1} , whose sensitivity is at a higher altitude at 30 hPa and above, the warm air is not obvious (not shown), suggesting the top of the umbrella clouds might be below 30 hPa. One more noticeable feature is the wave pattern, which is more obvious in the upper part of Figure 2 and near the center from both stratospheric sounding channels, demonstrating the capability to use CrIS to detect the gravity wave generated from this strong volcano eruption.

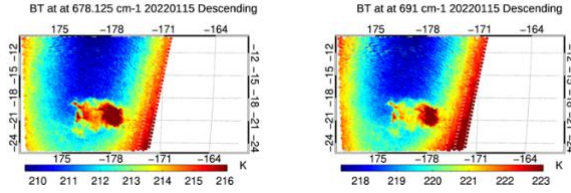


Figure 2 The BTs from CrIS measurement at channel 678.25 cm^{-1} (with the most energy from ~100-5 hPa and channel 691 cm^{-1} (sensitive to lower altitude than 678.25 cm^{-1}).

3.2. Upward movement of plume estimated from the observation of S-NPP and JPSS-1 in 50 minutes

To further check the westward and upward propagation of the plume, we compared the change of BT at $11.1\text{ }\mu\text{m}$ (BT11) in ~ 50 minutes apart between the observations of S-NPP and J-1. Figure 2 shows the difference of BT11 from CrIS on JPSS-1 (12:30 UTC) and S-NPP (13:20 UTC) after making the math-up to closest points. Indeed, the BT increases by ~5K over the upper umbrella cloud (UB) region while the BT over the lower umbrella cloud (UA) has little change, and there is a tendency of increase in the edge of the west. The change of BT11 is also evident from the histogram, where the 1st peak corresponds to UA that is almost the same, while 2nd peaks corresponds to UB and the observation from JPSS-1, in ~ 50 minutes later, is warmer than the observation from S-NPP. These results indicate the rapid upward movement of the plume even in 8-9 hours after the eruption, particularly the upper plume that is shooting to the middle stratosphere. As the stratosphere is

thermally stable (i.e., temperature increases with height), therefore, the buoyancy effect provides a favorable environment for the upward propagation. However, the lower umbrella cloud top is near the tropopause, which may serve as a barrier to limit its upward movement. From the temperature profile of ERA5 (not shown here), the increase of upper plume height in this 50 minutes is roughly ~ 1-2 km.

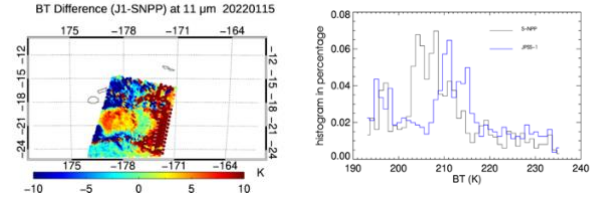
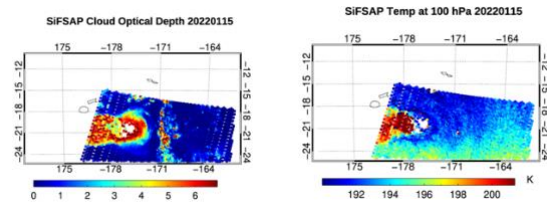


Figure 3 Map of the difference of BT at $11.1\text{ }\mu\text{m}$ from CrIS on JPSS-1 (12:30 UTC) minus S-NPP (13:20 UTC) (left), and histogram of BT at $11.1\text{ }\mu\text{m}$ in the region over the volcanic umbrella clouds.

3.3. Impact to the temperature, water vapor and O_3

From the SiFSAP retrieved temperature profiles, the tropopause is at ~ 100 hPa, so Figure 4 plots the map of the retrieved the temperature, water mixing ratio (H_2O) and ozone at 100 hPa. The cloud optical depth is also plotted as well, and the spatial resolution is ~14 km at nadir. Some pixels are missing over the lower umbrella cloud region due to the bad quality of retrievals. As expected, the cloud over the volcano and its west regions is thick with the optical depth of 4-7. The air temperature over upper umbrella cloud is warm, and the enhancement of water vapor associated with the exceptional water vapor ejection from the volcanic eruption is evident. However, there is only some slight increase of O_3 over the plume, together with the decrease of O_3 in the outer periphery of umbrella clouds, and the reason is under further investigation.



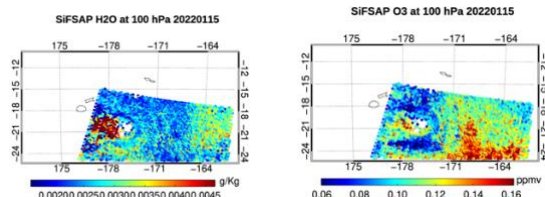


Figure 4 SIFSAP retrieved cloud optical depth, temperature, water mixing ratio (H₂O) and ozone at 100 hPa using CrIS and ATMS onboard JPSS-1.

4. SUMMARY AND CONCLUSION

Even after 8-9 hours following the strongest eruption of HTHH on 15 January 2022, a big area of plume and volcano clouds are captured using CrIS on S-NPP and JPSS-1 (or NOAA-20) in the nighttime. Using these hyper-spectra acquired by CrIS, we have shown some unique characteristics of these spectra, i.e. the upside down “U” feature for the spectra near 9.6 μm that is associated with the umbrella clouds or plume exceeding near tropopause and in the stratosphere. This special feature could be very useful for detecting the high clouds with the tops near or over tropopause during the night time and can have more other applications that is still under investigated.

Two layers of umbrella clouds can be identified even 8-9 hours after the big eruption, and the upper cloud is at stratosphere and associated with the westward propagation of the volcano plume. The increase of height of plume in the stratosphere can be estimated from two observations from S-NPP and JPSS-1 in 50 minutes apart, which can be up to 1-2 km.

Using a single field-of-view retrieval product, SiFSAP, from hyperspectral infrared sounder CrIS on JPSS-1, we analyzed the distribution of the retrieved cloud optical depth, temperature, water vapor and O₃ products. We have shown that the cloud is thick with optical depth of 4-6, and confirmed the unprecedented ejection of water vapor to the stratosphere from HTHH. This study demonstrates the value of hyperspectral infrared sounder and single-field-view products for monitoring the volcanic eruption, and further study of its impact on climate using SIFSAP and model data is on-going.

5. REFERENCES

[1] Carn SA, Krotkov NA, Fisher BL and Li C (2022), Out of the blue: Volcanic SO₂ emissions during the 2021–2022 eruptions of Hunga Tonga—Hunga Ha’apai (Tonga). *Front. Earth Sci.* 10:976962. doi: 10.3389/feart.2022.976962

[1] Carr, J. L., Horvath, ..., Wu, D. L., & Friberg, M. D. (2022). Stereo plume height and motion retrievals for the

record-setting Hunga Tonga-Hunga Ha’apai eruption of 15 January 2022. *Geophysical Research Letters*, 49, e2022GL098131. <https://doi.org/10.1029/2022GL098131>

[2] Millán, L., Santee, M. L., Lambert, A., Livesey, N. J., Werner, F., Schwartz, M. J., et al. (2022), The Hunga Tonga-Hunga Ha’apai hydration of the stratosphere. *Geophys. Res. Lett.*, 49, e2022GL099381, <https://doi.org/doi:10.1029/2022GL099381>

[3] Fleming, E. L., Newman, P. A., Liang, Q., & Oman, L. D. (2024). Stratospheric temperature and ozone impacts of the Hunga Tonga-Hunga Ha’apai water vapor injection. *Journal of Geophysical Research: Atmospheres*, 129, e2023JD039298, <https://doi.org/10.1029/2023JD039298>

[4] Schoeberl, M.R.; Wang, Y.; Ueyama, R.; Taha, G.; Jensen, E.; Yu, W. Analysis and impact of the Hunga Tonga-Hunga Ha’apai stratospheric water vapor plume. *Geophys. Res. Lett.* **2022**, 49, e2022GL100248.

[5] Christopher D. Barnet. et al., “The NOAA Unique CrIS/ATMS Processing System (NUCAPS): Algorithm Theoretical Basis Documentation,” https://star.nesdis.noaa.gov/jpss/documents/ATBD/ATBD_NUCAPS_v3.1.pdf, 2021

[6] Smith, N., Barnet, C.D., “Uncertainty Characterization and Propagation in the Community Long-Term Infrared Microwave Combined Atmospheric Product System (CLIMCAPS),” *Remote Sens.*, vol. 11, pp. 1227, 2019

[7] M. Goldberg and L. Zhou, “The joint polar satellite system — Overview, instruments, proving ground and risk reduction activities,” *2017 IEEE International Geoscience and Remote Sensing Symposium (IGARSS)*, Fort Worth, TX, 2017, pp. 2776-2778, doi: 10.1109/IGARSS.2017.8127573.

[8] Gupta, A. K., Bennartz, R., Fauria, K. E., and Mittal, T. (2022). Timelines of plume characteristics of the Hunga Tonga-Hunga Ha’apai eruption sequence from 19 December 2021 to 16 January 2022: Himawari-8 observations. *Earth Space Sci. Open 'rchive*. doi:10.1002/essoar.10510853.2.

[9] Liu, X., W. L. Smith, D. K. Zhou, and A. Larar, “Principal component-based radiative transfer model for hyperspectral sensors: theoretical concept,” *Appl. Opt.* 45, 201-209, 2006.

[10] Wu, W, X. Liu, D. K. Zhou, A. Larar, Q. Yang, and S. Kizer, , Q. Liu: The Application of PCRTM Physical Retrieval Methodology for IASI Cloudy Scene Analysis. *IEEE Transactions on Geoscience and Remote Sensing*. PP. 1-15. 10.1109/TGRS.2017.2702006, 2017.

[11] Wu, W. X. Liu, X. Xiong, Q. Yang, A. Lara, D. K. Zhou, 2022: Single Field-of-view Sounding Atmospheric Products. 2022 *IEEE International Geoscience and Remote Sensing Symposium (IGARSS)*.

[12] Ghazi, A. Nimbus 4 Observations of Changes in Total Ozone and Stratospheric Temperature during a Sudden Warming. *J. Atmos. Sci.* 1974, 31, 2197–2206

[13] Xiong, X.; Liu, X.; Wu, W.; Knowland, K.E.; Yang, F.; Yang, Q.; Zhou, D.K. Impact of Stratosphere on Cold Air Outbreak: Observed Evidence by CrIS on SNPP and Its Comparison with Models. *Atmosphere* 2022, 13, 876. <https://doi.org/10.3390/atmos13060876>